

1 RESEARCH ARTICLES

2

3 Title: MOLECULAR AND MORPHOLOGICAL DIVERSITY OF *TREBOUXIA*
4 MICROALGAE IN SPHAEROTHALLIOID *CIRCINARIA* SPP. LICHENS ¹

5

6 Authors: Arántzazu Molins ^{2,†}, Patricia Moya [†], Francisco J. García-Breijo, José Reig-
7 Armiñana and Eva Barreno.

8

9 Arántzazu Molins: Botánica, ICBIBE and Jardí Botànic. Fac. CC. Biológicas, Universitat de
10 València, C/ Dr. Moliner, 50. 46100-Burjassot, Valencia, Spain.

11 Patricia Moya: Botánica, ICBIBE and Jardí Botànic. Fac. CC. Biológicas, Universitat de
12 València, C/ Dr. Moliner, 50. 46100-Burjassot, Valencia, Spain.

13 Francisco J. García-Breijo: Dpto. Ecosistemas Agroforestales, Universitat Politècnica de
14 València, Camino de Vera s/n. 46022-Valencia, Spain.

15 José Reig-Armiñana: Botánica, ICBIBE and Jardí Botànic. Fac. CC. Biológicas, Universitat
16 de València, C/ Dr. Moliner, 50. 46100-Burjassot, Valencia, Spain.

17 Eva Barreno: Botánica, ICBIBE and Jardí Botànic. Fac. CC. Biológicas, Universitat de
18 València, C/ Dr. Moliner, 50. 46100-Burjassot, Valencia, Spain.

19

20 ¹ Date of submission and acceptance

21 ² For correspondence: A. Molins, Phone number: +34 963544376, Fax number +34
22 963544082, email: arantxa.molins@uv.es.

23 [†] These two authors contributed equally to this work.

24 **Running Head:** *Trebouxia* diversity in *Circinaria*

25

26 **ABSTRACT**

27 Three vagrant (*Circinaria hispida*, *Circinaria gyrosa*, *Circinaria* sp. '*paramerae*') and one
28 crustose (semi-vagrant, *Circinaria* sp. '*oromediterranea*') growing in very continental areas in
29 the Iberian Peninsula were selected to study the phycobiont diversity. Mycobiont
30 identification was checked using nrITS DNA barcoding: *Circinaria* sp. '*oromediterranea*' and
31 *Circinaria* sp. '*paramerae*' formed a new clade. Phycobiont diversity was analyzed in 50
32 thalli of *Circinaria* spp. using nrITS DNA and LSU rDNA, with microalgae coexistence being
33 found in all the species analyzed by Sanger sequencing. The survey of phycobiont diversity
34 showed up to four different *Trebouxia* spp. as the primary phycobiont in 20 thalli of *C.*
35 *hispida*, in comparison with the remaining *Circinaria* spp. where only one *Trebouxia* was the
36 primary microalga. In lichen species showing coexistence, some complementary approaches
37 are needed (454 pyrosequencing and/or ultrastructural analyses). Five specimens were
38 selected for HTS analyses: 22 *Trebouxia* OTUs were detected, ten of them not previously
39 known. TEM analyses showed three different cell morphotypes (*Trebouxia* sp. OTU A12,
40 OTU S51 and *T. cretacea*) whose ultrastructure is described here in detail for the first time.
41 HTS revealed a different microalgae pool in each species studied, and we cannot assume a
42 specific pattern between these pools and the ecological and/or morphological characteristics.
43 The mechanisms involved in the selection of the primary phycobiont and the other microalgae
44 by the mycobiont are unknown, and require complex experimental designs. The systematics
45 of the genus *Circinaria* is not yet well resolved, and more analyses are needed to establish a
46 precise delimitation of the species.

47

48 **KEY WORDS**

49 Coexistence, 454-pyrosequencing, Sanger-sequencing, *Trebouxia*, ultrastructure, vagrant-
50 lichen

51

52

53

54 **INTRODUCTION**

55 Lichens living unattached to a substrate are commonly known as ‘vagrant’ or ‘vagant’ growth-
56 forms. Rogers (1977) stated the term vagrant for the obligatory unattached lichens, and
57 ‘erratic’ for the facultative attached, that are primarily crustose to soil or stones, and during
58 the latest stages of their ontogeny are partially vagrant or semi-vagrant. Several authors
59 applied these concepts to refer to this peculiar ways of life (Crespo and Barreno 1978,
60 Rosentreter 1993, Sohrabi et al. 2013). Vagrant and erratic lichens have been reported for
61 every continent in the world, they appear to be characteristic of arid and semiarid areas and
62 tend to be concentrated in regions of continental weather, high irradiation and persistent winds
63 (Weber 1977, Büdel and Wessels 1986, Hafellner et al. 2004, Sánchez et al. 2014).

64 According to Sohrabi et al. (2013), in *Circinaria*, sphaerothallioid species are frequently
65 reported from continental semiarid deserts and arid and mountainous cold steppes. These taxa
66 show a Holarctic distribution pattern, being widespread in the Irano-Turanian region in Asia,
67 the Mediterranean region in North Africa and southern Europe, as well as the Madrean region
68 in North America (sensu Takhtajan 1986). In the Iberian Peninsula, sphaerothallioid
69 *Circinaria* spp. are distributed in most continental regions, and can be found in central and
70 northern plateaus ‘Parameras’ as well as in different zones of the Iberian Mountain System.
71 These areas, between 900 and 2000 m a.s.l., are located between the supra- and the oro-
72 mediterranean bioclimatic belts, with open structured forests of *Juniperus* spp. and *Pinus* spp.

73 in mosaic with cushiony shrub and shrub-grassland communities, landscapes with similar
74 appearance to those of typical cold steppes (Barreno 1991, Breshears 2008, Rivas-Martínez et
75 al. 2011). The soils of these areas are subjected to cryoturbation processes that favor the
76 development of diverse vagrant or erratic lichen communities (Crespo and Barreno 1978).
77 Phycobiont molecular identification in lichens is traditionally performed using Sanger
78 sequencing that provides invaluable information in population analyses studies. Over the last
79 few decades, intrathalline microalgal coexistence has been proved in several lichen species
80 (Blaha et al. 2006, Ohmura et al. 2006, Piercey-Normore 2006, Muggia et al. 2010, 2014,
81 Casano et al. 2011, Molins et al. 2013, Leavitt et al. 2015). Lichen specimens analyzed by
82 Sanger sequencing showing high variability in their phycobiont preference, or coexistence
83 (double peaks in the electrophoretograms) should be studied using different techniques. HTS
84 approaches supply amounts of information to evaluate species diversity at diverse taxonomic
85 levels. These HTS techniques have been progressively applied in lichenological studies, and
86 provide much higher resolution to reveal the microalgae multiplicity associated with the
87 lichen thalli (Meiser et al. 2014, U'Ren et al. 2014, Park et al. 2015, Moya et al. 2017).
88 The majority of molecular studies in sphaerothallioid lichens are focused on mycobiont
89 analyses, but phycobionts have been mostly ignored and are poorly known (Molins et al.
90 2018). Moreover, these sphaerothallioid lichen species are interesting candidates to analyze the
91 phycobiont diversity due to the different morphology and growth-forms which occur under
92 diverse ecological settings. For this purpose, we selected *Circinaria hispida* (Mereschk.) A.
93 Nordin, S. Savić and Tibell, *Circinaria gyrosa* Sohrabi, Sipman, V. John and V.J. Rico,
94 *Circinaria* sp. '*oromediterranea*' and *Circinaria* sp. '*paramerae*'. The aim of this study was to
95 reveal the microalgal diversity associated with different *Circinaria* lichen species by Sanger
96 sequencing, 454-pyrosequencing and ultrastructural techniques. We try to solve if the

97 microalgae taxa associated with the thalli change in two *C. hispida* from different locations
98 and if the phycobiont pool vary between the four *Circinaria* spp. with different morphologies
99 and habitat requirements.

100

101 **MATERIALS AND METHODS**

102 **Lichen material**

103 At least nine specimens of each *Circinaria* spp. were selected from three different locations.

104 *Circinaria hispida* (n=10) from Zaorejas (Guadalajara, Spain) (40°46'02'N, 2°11'40'W, 1105

105 m a.s.l.), *C. hispida* (n=10) and *Circinaria gyrosa* (n=11) from Maranchón (Guadalajara,

106 Spain) (41°02'56'N, 2°21'35'W, 1196 m a.s.l.), and *Circinaria* sp. '*oromediterranea*' (n=10)

107 (40°05'48'N, 1°01'28'W, 2010 m a.s.l.) and *Circinaria* sp. '*paramerae*' (n=9) (40°06'26'N,

108 1°01'18'W, 1925 m a.s.l.) from the Javalambre Mountain summits (Teruel, Spain). Samples

109 were dried out for one day and then stored at -20 °C until processing.

110 **Sample preparation, DNA extraction, amplification and Sanger sequencing**

111 Lichen thalli were examined under a stereo-microscope to remove surface contamination and

112 were sterilized by sequential immersion in ethanol and NaOCl (Arnold et al. 2009).

113 Fragments from different parts of the thalli were randomly excised and pooled together.

114 Total genomic DNA from all the samples was isolated and purified using the DNeasy™

115 Plant Mini kit (Qiagen, Hilden, Germany) following the manufacturer's instructions.

116 Phycobiont locus encoding the nrITS DNA (internal transcribed spacer) was amplified using

117 the primer pair nr-SSU-1780 (Piercey-Normore and DePriest 2001) and ITS4 (White et al.

118 1990). As a chloroplast genome marker, we studied a region of the LSU rRNA gene by using

119 the algal-specific primers 23SU1 and 23SU2 (del Campo et al. 2010). Fungal nrITS DNA was

120 amplified using the primer pair ITS1F (Gardes and Bruns 1993) and ITS4 (White et al. 1990).
121 PCR reactions were performed as described in Molins et al. (2018) (Table 1).

122 **454-pyrosequencing analyses**

123 One representative specimen of each *Circinaria* spp. was selected and pyrosequenced
124 following the protocol described in Moya et al. 2017. Two sequencing runs were performed in
125 this study. The first run was performed on a plate comprising of 82 multiplex identifiers
126 (MIDs) including *C. hispida* (Zaorejas and Marachón) and *Circinaria* sp. '*paramerae*'. The
127 second run was performed on a plate comprising of 24 MIDs, which included *C. gyrosa* and
128 *Circinaria* sp. '*oromediterranea*'.

129 The RT-PCRs and PCRs were performed and purified as previously described in Moya et al.
130 (2017) as mentioned in these protocol we performed as technical replicate each PCR by
131 triplicate. The number of cycles of PCR I and PCR II were determined by the average Ct
132 (cycle threshold) of the RT-PCR I and RT-PCR II (Ct PCR I: *C. hispida* from Zaorejas 21, *C.*
133 *hispida* from Maranchón 24, *C. sp. 'paramerae'* 19, *C. sp. 'oromediterranea'* 19 and *C.*
134 *gyrosa* 19 and Ct PCR II: *C. hispida* from Zaorejas 19, *C. hispida* from Maranchón 10, *C. sp.*
135 '*paramerae*' 8, *C. sp. 'oromediterranea'* 8 and *C. gyrosa* 8). Algal nrITS DNA sequences
136 were determined using a GS Junior 454 system (Roche 454 Life Sciences, Branford, CT,
137 USA) following the Roche Amplicon Lib-L protocol at the Genomics Core Facility at the
138 University of Valencia (Spain). Reads were processed as described in Moya et al. (2017) and
139 clustered based on S 99 -L 0.9 criteria. The consensus sequences of the OTUs were identified
140 using the BLAST tool in the GenBank data base (Altschul et al. 1990), and were encoded as
141 *C. spp._number of OTU_number of sequences* (Table 1).

142 **Phycobiont phylogenetic analysis of sequences obtained by Sanger sequencing and 454-**
143 **pyrosequencing.**

144 For the nrITS DNA a multiple alignment was prepared including: i) the phycobiont obtained
145 by Sanger sequencing, ii) the consensus sequence OTUs (operational taxonomic units)
146 obtained by 454-pyrosequencing analysis, iii) selected sequences described by Leavitt et al.
147 (2015), and iv) a selection of *Trebouxia* species available from the Culture Collection of
148 Algae at Göttingen University (SAG), from the Culture Collection of Algae at the University
149 of Texas (UTEX) and *Trebouxia* sp. TR9 (Casano et al. 2011). We included *Trebouxia*
150 *corticola* (AJ249566) as the outgroup. The alignment was carried out using MAFFT v 7.0
151 (Katoh et al. 2002, Katoh and Toh 2008) using default parameters. The best-fit substitution
152 model for this region (GTR+G) was chosen using jModelTest v 2.0 (Darriba et al. 2012), and
153 by applying the Akaike Information Criterion (Akaike 1974). Maximum likelihood (ML)
154 analysis was implemented in RAxML v 8.1.11 (Stamatakis 2006) using the GTRGAMMA
155 substitution model. Bootstrap support was calculated based on 1,000 replications (Stamatakis
156 et al. 2008). Bayesian inferences (BI) were carried out in MrBAYES v 3.2 (Ronquist et al.
157 2012). Settings included two parallel runs with six chains over 20 million generations starting
158 with a random tree, and sampling after every 200th step. We discarded the first 25% of data as
159 burn-in. MAFFT, jModelTest, ML and BI analyses were implemented at the CIPRES Science
160 Gateway v 3.3 webportal (Miller et al. 2010). Phylogenetic trees were visualized in FigTree v
161 1.4.1 (Rambaut 2012).

162 In the case of the chloroplast genome marker, a multiple alignment was prepared including
163 the phycobiont obtained by Sanger sequencing and the selection of *Trebouxia* species
164 available from SAG, UTEX and *Trebouxia* sp. TR9. We included *Trebouxia corticola*
165 (AJ249566) as the outgroup. The alignment and phylogenetic analysis was carried out as
166 previously described for the nrITS DNA. The best-fit substitution model for this region was
167 GTR+I+G.

168 **Microscopic examinations**

169 For TEM (transmission electron microscope), the cells were fixed and dehydrated as
170 described in Molins et al. (2018). Samples were embedded in Spurr's resin according to the
171 manufacturer's instructions. Sections (90 nm) were cut and mounted as described in Moya et
172 al. (2018). The sections were observed with a JEOL JEM-1010 (80 kV) electron microscope,
173 equipped with a MegaView III digital camera and 'AnalySIS' image acquisition software.
174 TEM examinations were made at the SCSIE Service of the University of Valencia.

175 **Mycobiont phylogenetic analysis**

176 A multiple alignment was prepared including the newly determined fungal nrITS DNA
177 sequences from *Circinaria* spp. lichen thalli, and a selection of *Circinaria* spp. sequences
178 downloaded from the GenBank. *Lobothallia recedens* (HQ406807) were included as the
179 outgroup. The alignment and phylogenetic analysis was carried out as previously described
180 for the phycobiont.

181

182 **RESULTS**

183 **Mycobiont barcoding identification by Sanger sequencing**

184 The identities of *Circinaria gyrosa* mycobionts were confirmed by BLAST analyses against
185 the GenBank database. Significant matches of 100% identity and 99% coverage were
186 obtained respectively with *C. gyrosa* from Guadalajara (JQ797514) described by Sohrabi et
187 al. (2011, 2013). All sequences formed a well-supported clade (100/100) with the *C. gyrosa*
188 sequences included in the analysis (Fig. 1). The new *C. hispida* sequences from Zaorejas and
189 Maranchón matched into a clade including the *C. hispida* sequences downloaded from
190 Sohrabi et al. (2011, 2013) and the lectotype (HQ171235). *Circinaria* sp. '*oromediterranea*'

191 and *Circinaria* sp. '*paramerae*' appeared as two independent sister taxa in the phylogenetic
192 analyses, forming well-supported clades (99/100-80/100) in the mycobiont tree (Fig.1).

193 **Phycobiont identification by Sanger sequencing**

194 Two genome markers (nrITS DNA and LSU rRNA) were analyzed: only samples without
195 double peaks in the electrophoretogram for both genes were included in the study, the
196 remaining samples were removed from the analysis. The coexistence percentage detected by
197 Sanger ranged from 10% in *C. hispida* (Maranchón) to 100% in the case of *C. sp.*
198 '*oromediterranea*' (all specimens selected showed coexistence).

199 The phycobionts detected in *C. gyrosa* were grouped into a new well-supported clade
200 (100/100 nrITS DNA and 100/100 LSU rRNA) (Fig. 2 and Fig. S1). *C. sp. 'paramerae'*
201 sequences linked with *Trebouxia* sp. OTU A12 (KR913203, Leavitt et al. 2015) for nrITS
202 (Fig. 2) and *T. asymmetrica* for LSU rRNA (Fig. S1). Five of the nine specimens of *C. hispida*
203 Marachón matched with *Trebouxia* sp. OTU A12 (nrITS DNA)/*T. asymmetrica* (LSU rRNA),
204 and four with *T. cretacea* (nrITS DNA)/related to *T. asymmetrica* (LSU rRNA). In the case of
205 *C. hispida* Zaorejas, more variability was detected: 2 specimens showed *Trebouxia* sp. OTU
206 A12 (nrITS DNA)/*T. asymmetrica* (LSU rRNA), 1 *T. cretacea* (nrITS DNA)/related to *T.*
207 *asymmetrica* (LSU rRNA), 2 *T. asymmetrica* (nrITS DNA)/ *T. asymmetrica* (LSU rRNA) and
208 1 *Trebouxia* sp. OTU A63 (Leavitt et al. 2015) (nrITS DNA)/ related to *T. asymmetrica* (LSU
209 rRNA) (Fig. 2 and Fig. S1).

210 **Phycobiont diversity by 454-pyrosequencing**

211 One specimen per each *Circinaria* spp. was selected for the pyrosequencing analysis
212 (indicated in the phylogenetic trees as 454, Fig. 1, Fig. 2 and Fig. S1). Sequencing of nrITS
213 DNA amplicons produced 3,029 sequence reads for *C. hispida* (1,427 reads from Maranchón
214 and 1,602 from Zaorejas), 4,779 for *C. gyrosa*, 1,997 for *Circinaria* sp. '*paramerae*' and

215 5,508 for *Circinaria* sp. '*oromediterranea*'. Raw read datasets obtained from the five thalli
216 were individually trimmed, and singletons (88: 45 from Maranchón and 43 from Zaorejas, 41,
217 36 and 64, respectively) and unreliable reads were filtered and removed.

218 Clustering these nrITS DNA amplicons with a 99% similarity cutoff, sixteen OTUs for *C.*
219 *gyrosa*, nine OTUs for *Circinaria* sp. '*paramerae*', five for *C. hispida* and seventeen for
220 *Circinaria* sp. '*oromediterranea*' were recognized. The analyses of these five thalli detected a
221 total of 32 OTUs, which were representative of different phycobiont genera (*Trebouxia*,
222 *Asterochloris*, *Elliptochloris* and *Chlorophyta*).

223 *Trebouxia*

224 The aligned algal ITS1-5.8S was 312 bp in length. A total of 22 *Trebouxia* OTUs were
225 detected in the five analyzed thalli, six correspond to well-accepted *Trebouxia* species (*T.*
226 *decolorans*, *T. solaris*, *T. asymmetrica*, *T. cretacea*, *T. vaga* AV091 and AV092), one to
227 *Trebouxia* sp. TR9 and five to *Trebouxia* OTUs described by Leavitt et al. (2015) (S2, S8,
228 A12, A18 and A21) (Table 2). The ten newly detected OTUs (highlighted in grey in the
229 phylogenetic tree, Fig. 2, Table 2) were named as I51, I52, S51, S52 and A57 to A62
230 following the coding established by Leavitt et al. (2015) and Moya et al. (2017).

231 A total of four OUT's were detected in *C. hispida*. Among three from the thallus collected in
232 Marachón and two from Zaorejas, only *T. cretacea* was present in both thalli. The primary
233 phycobiont detected by Sanger sequencing from *C. hispida* Marachón (*T. cretacea*) matched
234 with the most abundant OTU obtained by pyrosequencing (Table 2). The new OTU A57 was
235 detected in this thallus. However, in *C. hispida* Zaorejas both sequences did not match, with
236 OTU A12 being the primary phycobiont by Sanger and *T. cretacea* by pyrosequencing (Fig. 2,
237 Table 2).

238 The primary phycobiont identified by Sanger in *C. gyrosa* fitted with the most abundant OTU
239 sequenced by 454-pyrosequencing: the new OTU S51. Four of the eleven OTUs detected by
240 the HTS approach were not previously detected: I51, S51, S52 and A60 (Fig. 2, Table 2).

241 In *Circinaria* sp. '*paramerae*' the primary phycobiont detected by Sanger and the most
242 abundant OTU pyrosequenced matched with A12. Also, two of the six OTUs detected by HTS
243 (OTUs I52 and A57) were not previously known (Fig. 2, Table 2).

244 The most abundant OTU analyzed by 454-pyrosequencing in *Circinaria* sp.

245 '*oromediterranea*' was A12. We were not able to identify the primary phycobiont by Sanger.

246 Six of the thirteen OTUs detected did not match with any described *Trebouxia* spp. (OTUs

247 I51, A58, A59, A60, A61 and A62) (Fig. 2, Table 2).

248 *Asterochloris*

249 Only 10 *Asterochloris* sequence reads were found in *C. gyrosa*, *Circinaria* sp. '*paramerae*'
250 and *Circinaria* sp. '*oromediterranea*'. The aligned algal ITS1-5.8S was 154 bp in length.

251 *Circinaria* sp. '*paramerae*' OTU9_4 and *Circinaria* sp. '*oromediterranea*' OTU14_4 were

252 related to *A. mediterranea* (KP257366). However, *C. gyrosa* OTU12_2 was not related to any

253 previously described *Asterochloris* taxon (phylogeny not shown) (Table 3).

254 *Elliptochloris* and *Chlorophyta*

255 Sequence reads of additional green algae genera were obtained from *Circinaria* sp.

256 '*oromediterranea*' and *C. gyrosa*. In both lichen species, we clustered 7 OTUs (4 in

257 *Circinaria* sp. '*oromediterranea*' and 3 from *C. gyrosa*). Only 3 of them produced BLAST

258 matches with 96%-100% identity and 89%-100% coverage with *Elliptochloris subsphaerica*

259 and *Chlorophyta* sp. URa19. The remaining OTUs did not produce significant BLAST matches,

260 therefore, we could not assign them a taxon name (Table 3).

261 **Ultrastructural characterization of microalgae**

262 Transmission electronic microscopy (TEM) analyses of phycobionts based on the
263 ultrastructure of pyrenoids and plastids distinguished at least three different *Trebouxia*
264 morphotypes. Morphological characteristics of each morphotype in detail can be seen in Table
265 4 and in Figs 3-4-5.

266 One morphotype which was found in *C. gyrosa* cells (Fig. 3 A-B) showed a new pyrenoid
267 type (Py) with a horseshoe shape and abundant pyrenoglobuli (Pg). Thylakoid membrane
268 arrangement in the chloroplast (Chl) was dense with numerous plastoribosomes interspersed
269 and penetrating into the central pyrenoid zone.

270 The second morphotype was found in *Circinaria*. sp. '*oromediterranea*' (Fig. 3 C-D),
271 *Circinaria*. sp. '*paramerae*' (Fig. 4 A-B) and *C. hispida* from Zaorejas morphotype A cells
272 (Fig. 5 A-B). These cells presented a single central pyrenoid (Py) related to the
273 *gigantea/impressa* type described by Friedl (1989), with pyrenoglobuly (Pg) uniformly
274 distributed within the pyrenoid matrix. The thylakoid membrane disposition was dense and
275 grouped in stacks, shaped by three or four straight membranes.

276 The third morphotype was detected *C. hispida* from Maranchón (Fig. 4 C-D) and *C. hispida*
277 from Zaorejas morphotype B (Fig. 5 C-D) cells. They presented a new irregular and lobulated
278 pyrenoid type (Py) which did not fit with those described by Friedl (1989). Thylakoid
279 membranes penetrated and crossed the pyrenoid matrix. Chloroplast (Chl) alternated dense,
280 and with lower arrangements.

281

282 **DISCUSSION**

283 Previously results in Molins et al. (2018) detected, using 454-pyrosequencing, the coexistence
284 of two *Trebouxia* OTUs (*Trebouxia cretacea* and A12) in the *Circinaria hispida* thallus from
285 Zaorejas. These preliminary results raise further intriguing questions: i) If we increase the

286 number of specimens included by location, and analyze different *Circinaria* spp. using Sanger
287 sequencing, what survey of photobiont diversity will we obtain? ii) If we compare two *C.*
288 *hispidata* from different locations (Zaorejas vs. Marachón), does the microalgae taxa associated
289 with the thalli change? and iii) Does the intrathalline phycobiont taxa modify if we compare
290 five *Circinaria* thalli with different morphologies and ecological settings?

291 For this purpose, in this study we applied different molecular and morphological analyses to
292 study the phycobiont diversity in four taxa of *Circinaria*, which grow in continental Iberian
293 ecosystems: Sanger sequencing, 454-pyrosequencing and ultrastructural examinations.

294 i) Survey of phycobiont diversity obtained by Sanger sequencing in different *Circinaria* spp.

295 Only one primary phycobiont was detected by Sanger sequencing, except for *Circinaria* sp.
296 '*oromediterranea*' which showed electrophoretograms with double peaks and hence were
297 removed from the phylogenetic analysis (Muggia et al. 2014, Leavitt et al. 2015,
298 Voytsekhovich and Beck 2015). In lichen species that show coexistence, some complementary
299 approaches to Sanger sequencing are needed to determine the primary phycobiont. Due to the
300 frequent occurrence of the coexistence phenomenon, we suggest including molecular
301 identification and ultrastructural characterization when using phycobiont cultures in
302 physiological and biochemical studies.

303 Moreover, if two phycobionts are highly represented inside the thallus (i.e. *C. hispidata*
304 Zaorejas) Sanger sequencing could randomly amplify one of them. In this situation, the
305 combination of different techniques, both molecular and microscopic, are crucial to confirm
306 the presence of these two morphotypes related to the *Trebouxia* genus. Ultrastructural traits of
307 pyrenoids from cultured phycobionts have been traditionally used to characterize *Trebouxia*
308 species (Friedl 1989), and some authors have highlighted the suitability of the pyrenoid
309 structures for species delimitation by TEM (Ascaso and Galván 1976, Ascaso et al. 1986,

310 Brown et al. 1987, Catalá et al. 2016). TEM allowed us to define and corroborate the presence
311 of these different morphotypes, and also describe in detail the ultrastructure of *Trebouxia* sp.
312 OTU A12 and *T. cretacea*. Over recent years, *Trebouxia* molecular data have increased
313 dramatically, revealing substantial diversity within the genus. The combination of molecular
314 analyses together with ultra-structural techniques should be initiated to clarify taxonomic
315 concepts to delimit new taxa of microalgae, and particularly in the case of *Trebouxia* diversity
316 (Muggia et al. 2016, Moya et al. 2017, Molins et al. 2018) both in symbiotic and isolated
317 states.

318 The survey of phycobiont diversity showed up to four different *Trebouxia* spp. (*T. cretacea*,
319 *T. asymmetrica*, A12 and A63) as the primary photobiont in 20 thalli of *C. hispida*, in
320 comparison with the remaining *Circinaria* spp. where only one *Trebouxia* was the primary
321 microalga (*C. gyrosa*-S51 and *Circinaria*. sp 'paramerae'-A12).

322 ii) Microalgae taxa associated with *C. hispida* from different locations (Zaorejas vs.
323 Marachón). Despite the 454-pyrosequencing limitations described in Moya *et al.* 2017 (low-
324 coverage samples, the region selected, etc.), this approach represents a powerful and
325 complementary approach to traditional Sanger sequencing, and helped us to shed light on
326 microalgal coexistence. Both *C. hispida* from geographically distant areas with identical
327 ecological settings (approx. 60 kms separates Zaorejas from Maranchón) uniquely shared the
328 presence of *T. cretacea*. This result, linked with the results obtained in *C. hispida* for these
329 two locations, seems to indicate a different selection of the primary phycobiont in each thallus
330 from the microalgae pool available in both localities (Peksa and Škaloud 2011, Dupont et al.
331 2016).

332 iii) Morphological and ecological settings related with the intrathalline phycobionts pattern in
333 five *Circinaria* thalli. The presence of multiple algal species, and the different dominance of

334 one of them in each *Circinaria* spp., imply the selection for a particular algal OTU by the
335 mycobiont (Peksa and Škaloud 2011, Dupont et al. 2016). It is possible that different algal
336 communities will adapt to different types of lichen thalli in different environments, or under
337 specific environmental conditions (Zhang et al. 2015).

338 Unexpectedly for us, two vagrant *Circinaria* spp. (*C. gyrosa* and *C. hispida*) collected at the
339 same location, (Maranchón) showed a completely different pool of intrathalline microalgae
340 (Table 2). In this case, different lichen thalli under identical ecological settings held different
341 algal communities but, as mentioned before, *C. hispida* can vary its primary algal selection.

342 *Circinaria* sp. '*oromediterranea*' and *Circinaria* sp. '*paramerae*' were collected at the top of
343 the Javalambre Mountains (Teruel, Spain). *Circinaria* sp. '*oromediterranea*' was exclusively
344 found at the summit (2000-2020 m), under cryoro-mediterranean bioclimatic conditions with
345 high irradiation and constant winds. This specific area shows a community of cushiony
346 chamaephytes and grasses, where some plants are endemic, or related, to the flora of Eastern-
347 Mediterranean and Irano-Turanian mountains (Costa and Soriano 1999, Rivas-Martínez et al.
348 2011). *Circinaria* sp. '*paramerae*' is more widespread and frequent in Iberian Parameras, but
349 only below 1900 m (Barreno unpublished data). The specimen pyrosequenced, was also
350 collected in the Javalambre Mountains but down the summit, which belongs to a different
351 bioclimatic belt with creeping shrubs and grasses. These two different lichens only shared the
352 primary phycobiont *Trebouxia* OTU A12, the remaining twelve and five OTUs encountered,
353 respectively, were exclusive for each lichen thallus. While *Circinaria* sp. '*paramerae*' must be
354 considered as vagrant, *Circinaria* sp. '*oromediterranea*' should be termed crustose (semi-
355 vagrant) because these lichen thalli are exclusively linked to small pebbles rolling on the
356 ground (Crespo and Barreno 1978). Although this result should be further confirmed by more

357 detailed analyses, the microalgae pool available for each species could be determined by the
358 differences in growth-forms.

359 Although the aim of this study was not to discuss mycobiont identification, some conflicting
360 results have led to an interesting outcome. Molecular identification of lichenized fungi should
361 not be overlooked in phycobiont studies in order to corroborate lichen identification. While
362 the mycobionts of *C. gyrosa* were confirmed by the DNA barcoding proposed by Schoch et al.
363 (2012), nrITS DNA sequences from *Circinaria* sp. 'oromediterranea' and *Circinaria* sp.
364 'paramerae' formed a new clade which did not match any previously described *Circinaria*
365 spp. Provisional names have been proposed until they can be formally described:

366 'oromediterranea' refers to the environmental conditions at the summit of the Javalambre
367 Mountains, and 'paramerae' to the Iberian Parameras ecosystems. These two new lichen taxa
368 should be corroborated in studies including additional molecular markers. Despite the fact
369 that several mycological studies were focused on solving the taxonomic relationships in this
370 genus, this is still under revision and resulted in some controversial taxa such as *C. hispida*.
371 The variability observed in the *C. hispida* clade allows us to consider it as a complex, more
372 than a monophyletic taxon.

373 In conclusion, the microalgae pool is different in each of the species studied, and even varies
374 among thallus of the same species growing in different localities (*C. hispida* Maranchón vs
375 Zaorejas) and between two different species with an identical growing form in the same
376 locality (*C. gyrosa* and *C. hispida* Maranchón); there is no specific pattern. Moreover, two
377 different species with different growing forms in the same locality, but in different bioclimatic
378 belts (*Circinaria* sp. 'oromediterranea' and *Circinaria* sp. 'paramerae'), only share the
379 primary phycobiont. The mechanisms involved in the selection of the primary phycobiont and
380 the rest of microalgae by the mycobiont are unknown, and require complex experimental

381 designs. The systematics of the genus *Circinaria* is not yet well resolved, and more analyses
382 are needed to establish a precise delimitation of the species.

383

384 **ACKNOWLEDGEMENTS**

385 Supported by the Ministerio de Economía y Competitividad (MINECO, Spain) (CGL2016-
386 79158-P), Excellence in Research (Generalitat Valenciana, Spain) (PROMETEO/2017/039).

387 We want to thank the technicians (M^a Teresa Mínguez and Nuria Cebrián) from the Servicio
388 de Microscopía Electrónica, SCSIE and Jardí Botànic (Universitat de València) who helped us
389 to perform the TEM process, and Santiago Català for the pyrosequencing analyses. Daniel
390 Sheerin revised the English manuscript.

391

392 **REFERENCES**

393 Akaike, H. 1974. A new look at the statistical model identification. *IEEE Trans. Automat.*
394 *Control* 19: 716–723.

395 Altschul, S. F., Gish, W., Miller, W., Myers, E. W. & Lipman, D. J. 1990. Basic local alignment
396 search tool. *J. Mol. Biol.* 215: 403–410.

397 Arnold, A. E., Miadlikowska, J., Higgins, K. L., Sarvate, S. D., Gugger, P., Way, A.,
398 Hofstetter, V., Kauff, F. & Lutzoni, F. 2009. A phylogenetic estimation of trophic transition
399 networks for ascomycetous fungi: are lichens cradles of symbiotrophic fungal
400 diversification? *Syst. Biol.* 58: 283–297.

401 Ascaso, C. & Galván, J. 1976. The ultrastructure of the symbionts of *Rhizocarpon*
402 *geographicum*, *Parmelia conspersa* and *Umbilicaria pustulata* growing under dryness
403 conditions. *Protoplasma* 87: 409–418.

404 Ascaso, C., Brown, D. H. & Rapsch, S. 1986. The ultrastructure of the phycobiont of
405 desiccated and hydrated lichens. *Lichenologist* 18: 37–46.

406 Barreno, E. 1991. Phytogeography of terricolous lichens in the Iberian Peninsula and the
407 Canary Islands. *Botanika Chronika* 10: 199–210.

408 Blaha, J., Baloch, E. & Grube, M. 2006. High photobiont diversity associated with the
409 euryoecious lichen-forming ascomycete *Lecanora rupicola* (Lecanoraceae, Ascomycota).
410 *Biol. J. Linn. Soc.* 88: 283–293.

411 Breshears, D. 2008. Structure and function of woodland mosaics: consequences of patch-scale
412 heterogeneity and connectivity along the grassland-forest continuum. In: *Western North*
413 *America Juniperus communities. A dynamic vegetation type.* (Van Auken, O.W. ed). *Ecol.*
414 *Stud.* 196: 58–92.

415 Brown, D. H., Ascaso, C. & Rapsch, S. 1987. Ultrastructural changes in the pyrenoid of the
416 lichen *Parmelia sulcata* stored under controlled conditions. *Protoplasma* 136: 136–144.

417 Büdel, B. & Wessels, D. C. J. 1986. *Parmelia hueana* Gyeln. a vagrant lichen from the Namib
418 Desert, SWA Namibia. I: Anatomical and reproductive adaptations. *Dinteria* 18: 3–12.

419 del Campo, E. M., Gimeno, J., Casano, L.M., Gasulla, F., García-Breijo, F., Reig-Armiñana,
420 J., & Barreno, E. 2010. South European populations of *Ramalina farinacea* (L.) Ach. share
421 different *Trebouxia* algae. *Bibl. Lichenol.* 105:247–256. Casano L. M., del Campo E. M.,
422 García-Breijo F. J., Reig-Armiñana J., Gasulla F., del Hoyo A., Guéra, A. & Barreno, E.
423 2011. Two *Trebouxia* algae with different physiological performances are ever-present in
424 lichen thalli of *Ramalina farinacea*. Coexistence versus competition? *Environ. Microbiol.*
425 13:806–818.

426 Catalá, S., del Campo, E. M., Barreno, E., García-Breijo, F. J., Reig-Armiñana, J. & Casano,
427 L. M. 2016. Coordinated ultrastructural and phylogenomic analyses shed light on the

428 hidden phycobiont diversity of *Trebouxia* microalgae in *Ramalina fraxinea*. *Mol.*
429 *Phylogenet. Evol.* 94: 765–777.

430 Costa, M. & Soriano, P. 1999. Geobotanical excursion from Valencia to the Javalambre
431 summit. *Iter Ibericum.307727. Itinera Geobotanica.* 13: 69–79.

432 Crespo, A. & Barreno, E. 1978. Sobre las comunidades terrícolas de líquenes vagantes
433 (*Sphaerothallio-Xanthoparmelion vagantis* al. nov.). *Acta Bot. Malacit.* 4: 55–62.

434 Darriba, D., Taboada, G. L., Doallo, R. & Posada, D. 2012. jModelTest 2: more models, new
435 heuristics and parallel computing. *Nat. Methods* 9: 772–772.

436 Dupont, A., Griffiths, R. I., Bell, T. & Bass, D. 2016. Differences in soil micro-eukaryotic
437 communities over soil pH gradients are strongly driven by parasites and saprotrophs.
438 *Environ. Microbiol.* 18:2010–2014.

439 Friedl, T. 1989. Comparative ultrastructure of pyrenoids in *Trebouxia* (Microthamniales,
440 Chlorophyta). *Plant Syst. Evol.* 164: 145–159.

441 Gardes, M. and Bruns, T. D. 1993. ITS primers with enhanced specificity for basidiomycetes
442 application to the identification of mycorrhizae and rusts. *Mol. Ecol.* 2: 113–118.

443 Hafellner, J., Nimis, P. L. and Tretiach, M. 2004. New records of *Aspicilia hispida* from Italy
444 and Greece. *Herzogia* 17: 95–102.

445 Katoh, K., Misawa, K., Kuma, K. and Miyata, T. 2002. MAFFT: a novel method for rapid
446 multiple sequence alignment based on fast Fourier transform. *Nucleic Acids Res.* 30: 3059–
447 3066.

448 Katoh, K. and Toh, H. 2008. Recent developments in the MAFFT multiple sequence
449 alignment program. *Brief. Bioinform.* 9: 286–298.

450 Leavitt, S. D., Kraichak, E., Nelsen, M. P., Altermann, S., Divakar, P., Alors, D. Esslinger, T.
451 L., Crespo, A. & Lumbsch, T. 2015. Fungal specificity and selectivity for algae play a

452 major role in determining lichen partnerships across diverse ecogeographic regions in the
453 lichen-forming family Parmeliaceae (Ascomycota). *Mol. Ecol.* 24: 3779–3797.

454 Meiser, A., Bálint, M. & Schmitt I. 2014. Meta-analysis of Deep-sequenced fungal
455 communities indicates limited taxon sharing between studies and the presence of
456 biogeographic patterns. *New Phytol.* 201: 623–635.

457 Miller, M. A, Pfeiffer, W. & Schwartz, T. 2010. Creating the CIPRES Science Gateway for
458 inference of large phylogenetic trees. *Proceedings of the Gateway Computing
459 Environments Workshop* (GCE). New Orleans: LA, USA, pp. 1–8.

460 Molins, A., García-Breijo, F. J., Reig-Armiñana, J., del Campo, E. M., Casano, L. M. &
461 Barreno, E. 2013. Coexistence of different intrathalline symbiotic algae and bacterial
462 biofilms in the foliose Canarian lichen *Parmotrema pseudotinctorum*. *Vieraea* 41: 349–
463 370.

464 Molins, A., Moya, P., García-Breijo, F. J., Reig-Armiñana, J & Barreno, E. 2018. Assessing
465 lichen microalgal diversity by a multi-tool approach: isolation, Sanger sequencing, HTS
466 and ultrastructural correlations. *Lichenologist*, 50: 123–138.

467 Moya, P., Molins, A., Martínez-Alberola, F., Muggia, L. & Barreno, E. 2017. Unexpected
468 associated microalgal diversity in the lichen *Ramalina farinacea* is uncovered by
469 pyrosequencing analyses. *PloSOne*: DOI 101371/journal.pone.0175091.

470 Moya, P., Chiva, S., Molins, A., Jadrná, I., Škaloud, P., Peksa O. & Barreno, E. (2018).
471 *Myrmecia israeliensis* as the primary symbiotic microalga in squamulose lichens growing
472 in European and Canary Island terricolous communities. *Fottea*. (10.5507/fot.2017.022).

473 Muggia, L., Zellnig, G., Rabensteiner, J. & Grube, M. 2010. Morphological and phylogenetic
474 study of algal partners associated with the lichen-forming fungus *Tephromela atra* from
475 the Mediterranean region. *Symbiosis* 51: 149–160.

476 Muggia, L., Pérez–Ortega, S., Kopun, T., Zellnig, G. & Grube, M. 2014. Phycobiont
477 selectivity leads to ecological tolerance and evolutionary divergence in a polymorphic
478 complex of lichenized fungi. *Ann. Bot.* 114: 463–75.

479 Muggia, L., Leavitt, S. & Barreno, E. 2016. Report of the meeting of the *Trebouxia* working
480 group. In: Guzow- Krzeminska, [Ed.] *International Lichenological Newsletter*. pp. 35–37.

481 Nordin, A., Savić S. & Tibell L. 2010. Phylogeny and taxonomy of *Aspicilia* and
482 *Megasporaceae*. *Mycologia* 102: 1339–1349.

483 Ohmura, Y., Kawachi, M., Kasai, F., Watanabe, M. M. & Takeshita, S. 2006. Genetic
484 combinations of symbionts in a vegetatively reproducing lichen, *Parmotrema tinctorum*,
485 based on ITS rDNA sequences. *Briologist* 109:43–59.

486 Park, C. H., Kim, K. M., Elvebakk, A., Kim, O. S., Jeong, G. & Hong, S.G. 2015. Algal and
487 fungal diversity in Antarctic lichens. *J. Eukaryot. Microbiol.* 62: 196–205.

488 Peksa, O. & Škaloud, P. 2011. Do photobionts influence the ecology of lichens? A case study
489 of environmental preferences in symbiotic green alga *Asterochloris* (Trebouxiophyceae).
490 *Mol. Ecol.* 20: 3936–3948.

491 Piercey-Normore, M. D. & DePriest, P. T. 2001. Algal switching among lichen symbioses.
492 *Am. J. Bot.* 88: 1490–1498.

493 Piercey-Normore, M. D. 2006. The lichen-forming ascomycete *Evernia mesomorpha*
494 associates with multiple genotypes of *Trebouxia jamesii*. *New Phytol.* 169: 331–344.

495 Rambaut, A. 2012. *FigTree version 1.4.1*. <http://tree.bio.ed.ac.uk/software/figtree>.

496 Rivas-Martínez, S. et al. 2011. Mapa de series, geoserias y geopermaseries de vegetación de
497 España. [Memoria del mapa de vegetación potencial de España] Parte II. *Itinera Geobot.*
498 18: 5–800.

499 Rogers, R. W. 1977. Lichens of hot arid and semi-arid lands. In: Seaward, M. R. D. [Ed.]
500 *Lichen Ecology*. Academic Press, London, pp. 211–252.

501 Ronquist F., Teslenko, M., van der Mark, P., Ayres, D. L., Darling, A., Höhna, S., Larget, B.,
502 Liu, L., Suchard, M. A. & Huelsenbeck, J. P. 2012. MrBayes 3.2: Efficient Bayesian
503 phylogenetic inference and model choice across a large model space. *Systems Biol.* 61:
504 539–42.

505 Rosentreter, R. 1993. Vagrant lichens in North America. *Bryologist* 96: 333–338.

506 Sánchez, F. J., Meeßen J., Ruiz, M., Sancho, L.G., S. Ott, E., Vilchez, C., Hornek, G.,
507 Sadowsky, A. & de la Torre, R. 2014. UV-C tolerance of symbiotic *Trebouxia* sp. in the
508 space-tested lichen species *Rhizocarpon geographicum* and *Circinaria gyrosa*: role of the
509 hydration state and cortex/screening substances. *Int. J. Astrobiol.* 13: 1–18.

510 Schoch, C. L., Seifert, K. A., Huhndorf, S., Robert, V., Spouge, J. L., Levesque, C. A., Chen
511 W. & Fungal Barcoding Consortium 2012. Nuclear ribosomal internal transcribed spacer
512 (ITS) region as a universal DNA barcode marker for Fungi. *Proc. Nat. Acad. Sci.* 109:
513 6241–6246.

514 Sohrabi, M., Ahti, T. & Litterski, B. 2011. *Aspicilia digitata* sp. nov. a new vagrant lichen
515 from Kyrgyzstan. *Lichenologist* 43: 39–46.

516 Sohrabi, M., Stenroos, S., Myllys, L., Sochting, U., Ahti, T. & Hyvonen, J. 2013. Phylogeny
517 and taxonomy of the ‘manna lichens’. *Mycol. Prog.* 12: 231–269.

518 Stamatakis, A. 2006. RAxML-VI-HPC: maximum likelihood-based phylogenetic analyses
519 with thousands of taxa and mixed models. *Bioinformatics* 22: 2688–90.

520 Stamatakis, A., Hoover, P. & Rougemont, J. 2008. A rapid bootstrap algorithm for the RAxML
521 web servers. *Syst. Biol.* 57: 758–71.

- 522 Takhtajan, A. 1986. *Floristic Regions of the World*. University of California Press, Berkeley
523 and Los Angeles.
- 524 U'Ren, J. M., Riddle, J. M., Monacell, J. T., Carbone, I., Miadlikowska, J., & Arnold, A. E.
525 2014. Tissue storage and primer selection influence pyrosequencing-based inferences of
526 diversity and community composition of endolichenic and endophytic fungi. *Mol. Ecol.*
527 *Res.* 14:1032–1048.
- 528 Voytsekhovich, A. and Beck, A. 2015. Lichen phycobionts of the rocky outcrops of Karadag
529 massif (Crimean Peninsula). *Symbiosis* 68: 9–24.
- 530 Weber, W. A. 1977. Environmental modification and lichen taxonomy. In: Seaward, M. R. D.
531 [Ed.] *Lichen Ecology*. Academic Press, London, pp. 9–29.
- 532 White, T. J., Burns, T., Lee, S. & Taylor, J. 1990. *Amplification and direct sequencing of*
533 *fungus ribosomal DNA genes for phylogenetics*. Academic Press, Florida.
- 534 Zhang, T., Wei, X. L., Zhang, Y. Q., Liu, H.Y. & Yu, L. Y. 2015. Diversity and distribution of
535 lichen-associated fungi in the Ny-Ålesund Region (Svalbard, High Arctic) as revealed by
536 454 pyrosequencing. *Sci. Rep.* 5:10.1038/srep148.

537

538 **FIGURE LEGEND**

539 **Fig.1.** Phylogenetic analyses of nrITS DNA mycobiont from selected *Circinaria* spp. Values
540 at nodes indicate statistical support estimated by two methods: Maximum-likelihood bootstrap
541 and Bayesian inference posterior node probability. The newly obtained sequences were
542 designated by *. Accession numbers from *Circinaria* spp., and *Lobothallia recondens*
543 sequences retrieved from the GenBank accompany each species name. The specimen per each
544 *Circinaria* spp. selected for the pyrosequencing analyses were indicated in the phylogenetic

545 tree as 454. The scale bar shows the estimated number of substitutions per site.

546 **Fig.2.** *Trebouxia* phylogenetic analysis of *Circinaria* spp. Rooted ITS1-5.8S gene tree
547 representing 115 *Trebouxia* sequences, including 23 well-accepted *Trebouxia* species from
548 SAG and UTEX, *Trebouxia* sp. TR9 and 50 OTUs described by Leavitt *et al.* (2015) retrieved
549 from the GenBank. Pyrosequencing consensus sequences were encoded as *C.* spp._number of
550 OTU_number of sequences. Values at nodes indicate statistical support estimated by two
551 methods: Maximum-likelihood bootstrap and Bayesian inference posterior node probability.
552 Twenty-two *Trebouxia* OTUs detected in the pyrosequencing assay are indicated, and the nine
553 unknown OTUs are highlighted in grey. The specimen per each *Circinaria* spp. selected for the
554 pyrosequencing analyses were indicated in the phylogenetic trees as 454. Scale bar shows the
555 estimated number of substitutions per site.

556 **Fig. 3. A-B: *Circinaria gyrosa* and C-D: *Circinaria* sp. ‘*oromediterranea*’:** Cross section of
557 *C. gyrosa* and *C.* sp. ‘*oromediterranea*’ thallus by TEM. (A) Phycobionts of *C. gyrosa* inside
558 thallus (morphotype 1), (B) Detail of pyrenoid, (C) Phycobionts of *C.* sp. ‘*oromediterranea*’
559 inside thallus (morphotype 2), (D) Detail of pyrenoid. Abbreviations, Py (Pyrenoid), Pg
560 (Pyrenoglobuli), CW (Cell wall), SS (Secretory space), Chl (Chloroplast), PV (Peripheral
561 vesicles), CI (cytoplasmic inclusions), Hy (Hyphae). Bars 600 nm, 1 μ m and 2 μ m.

562 **Fig. 4. A-B: *Circinaria* sp. ‘*paramerae*’ and C-D: *Circinaria hispida* Maranchón.** Cross
563 section of *C.* sp. ‘*paramerae*’ and *C. hispida* from Maranchón thallus by TEM. (A)
564 Phycobionts of *C.* sp. ‘*paramerae*’ inside thallus (morphotype 2), (B) Detail of pyrenoid, (C)
565 Phycobionts of *C. hispida* from Maranchón inside thallus (morphotype 3), (D) Detail of
566 pyrenoid. Abbreviations, Py (Pyrenoid), Pg (Pyrenoglobuli), CW (Cell wall), SS (Secretory
567 space), Chl (Chloroplast), PV (Peripheral vesicles), CI (cytoplasmic inclusions), Hy
568 (Hyphae). Bars 500 nm, 800 nm, 1 μ m and 2 μ m.

569 **Fig. 5. A-D *Circinaria hispida* Zaorejas.** Cross section of *C. hispida* from Zaorejas by TEM .
570 (A) Morphotype 2 (A) of phycobionts found in *C. hispida* inside thallus (B) Detail of
571 pyrenoid, (C) Morphotype 3(B) of phycobionts in *C. hispida* inside thallus (D) Detail of
572 pyrenoid. Abbreviations, Py (Pyrenoid), Pg (Pyrenoglobuli), CW (Cell wall), SS (Secretory
573 space), Chl (Chloroplast), PV (Peripheral vesicles), CI (cytoplasmic inclusions), S (Starch
574 granules) Hy (Hyphae). Bars 600 nm, 800 nm and 2 μ m.

575

576 **SUPPORTING INFORMATION**

577 **Figure S1.** *Trebouxia* phylogenetic LSU rRNA analysis of *Circinaria* spp. Rooted tree
578 representing 25 *Trebouxia* sequences, including 18 well-accepted *Trebouxia* species from
579 SAG and UTEX and *Trebouxia* sp. TR9. Values at nodes indicate statistical support estimated
580 by two methods: Maximum-likelihood bootstrap and Bayesian inference posterior node
581 probability. The specimen per each *Circinaria* spp. selected for the pyrosequencing analyses
582 were indicated in the phylogenetic trees as 454. Scale bar shows the estimated number of
583 substitutions per site.

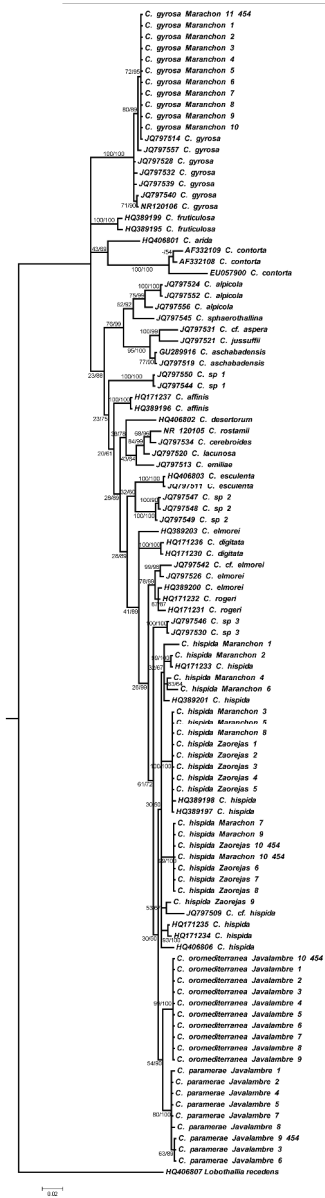
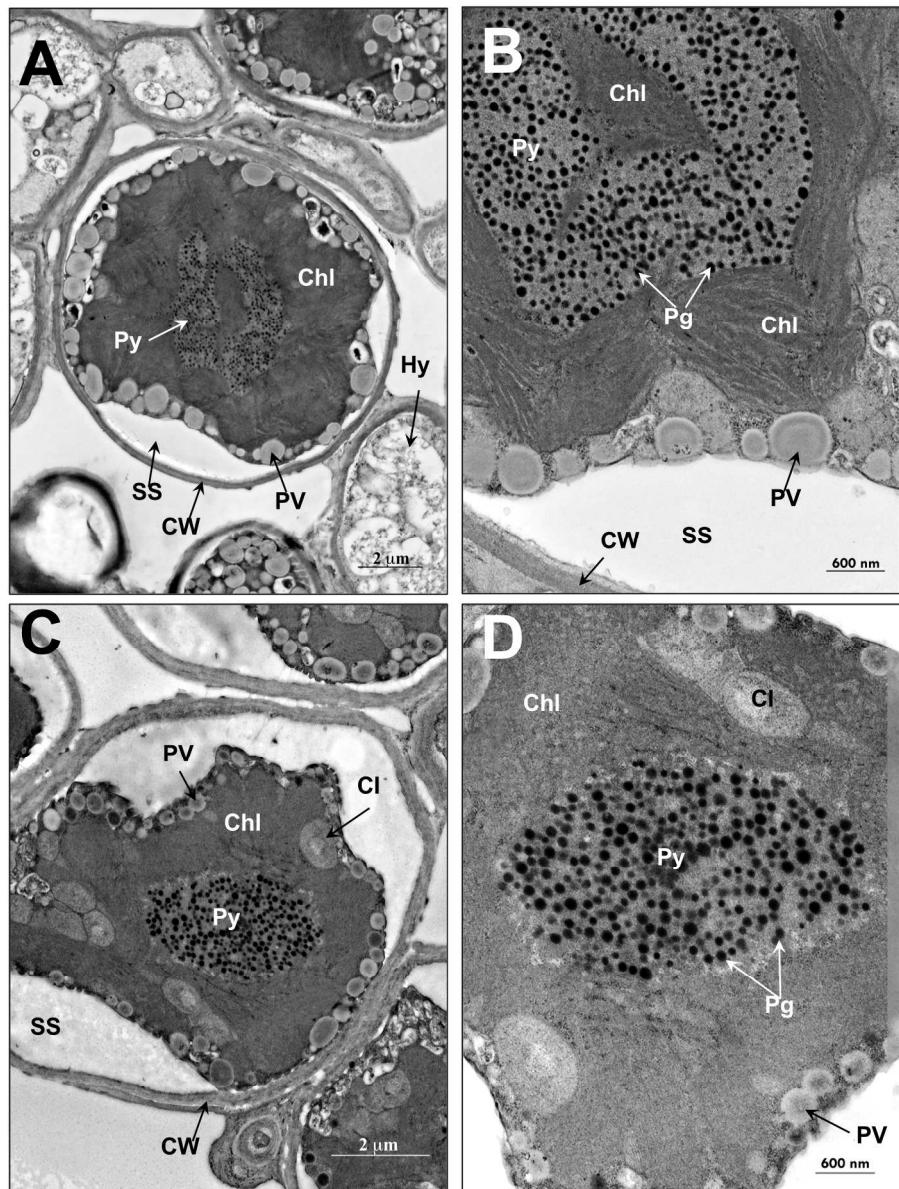
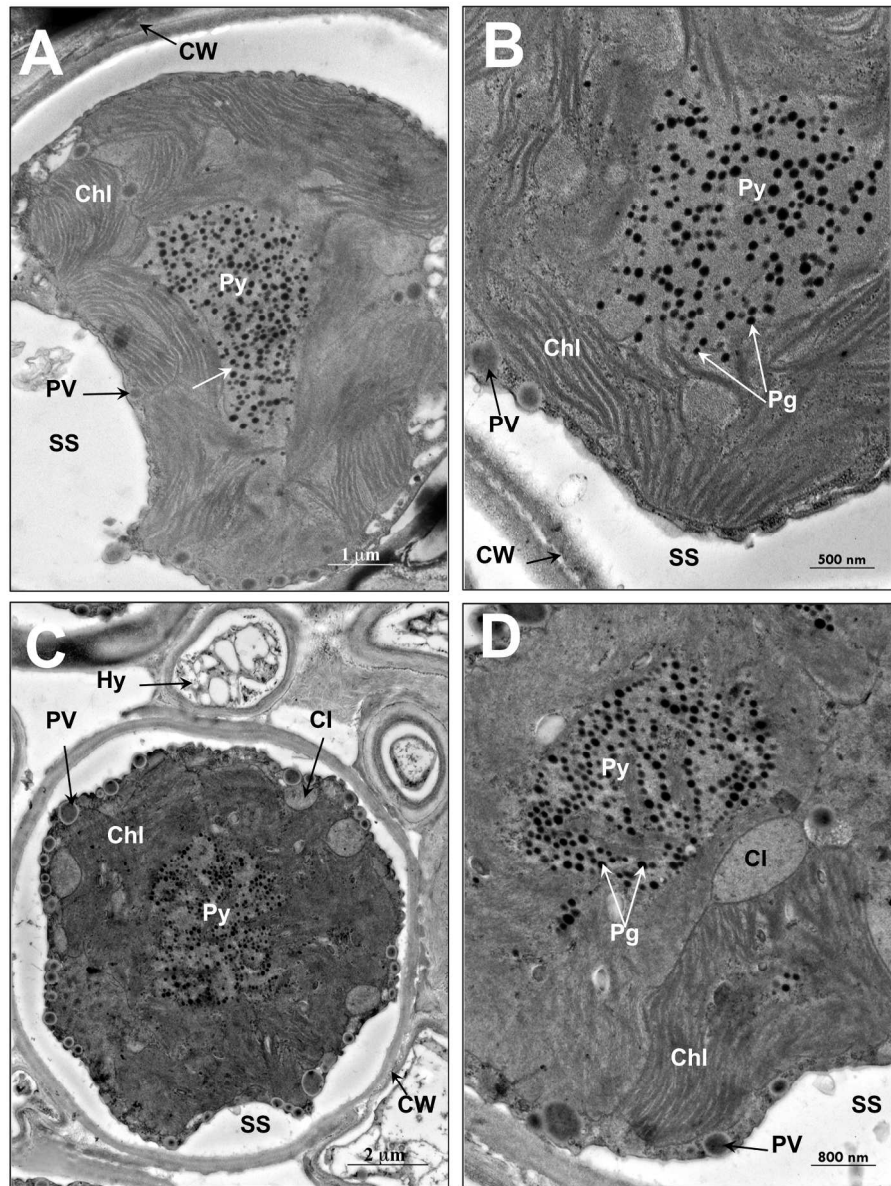


Fig 1

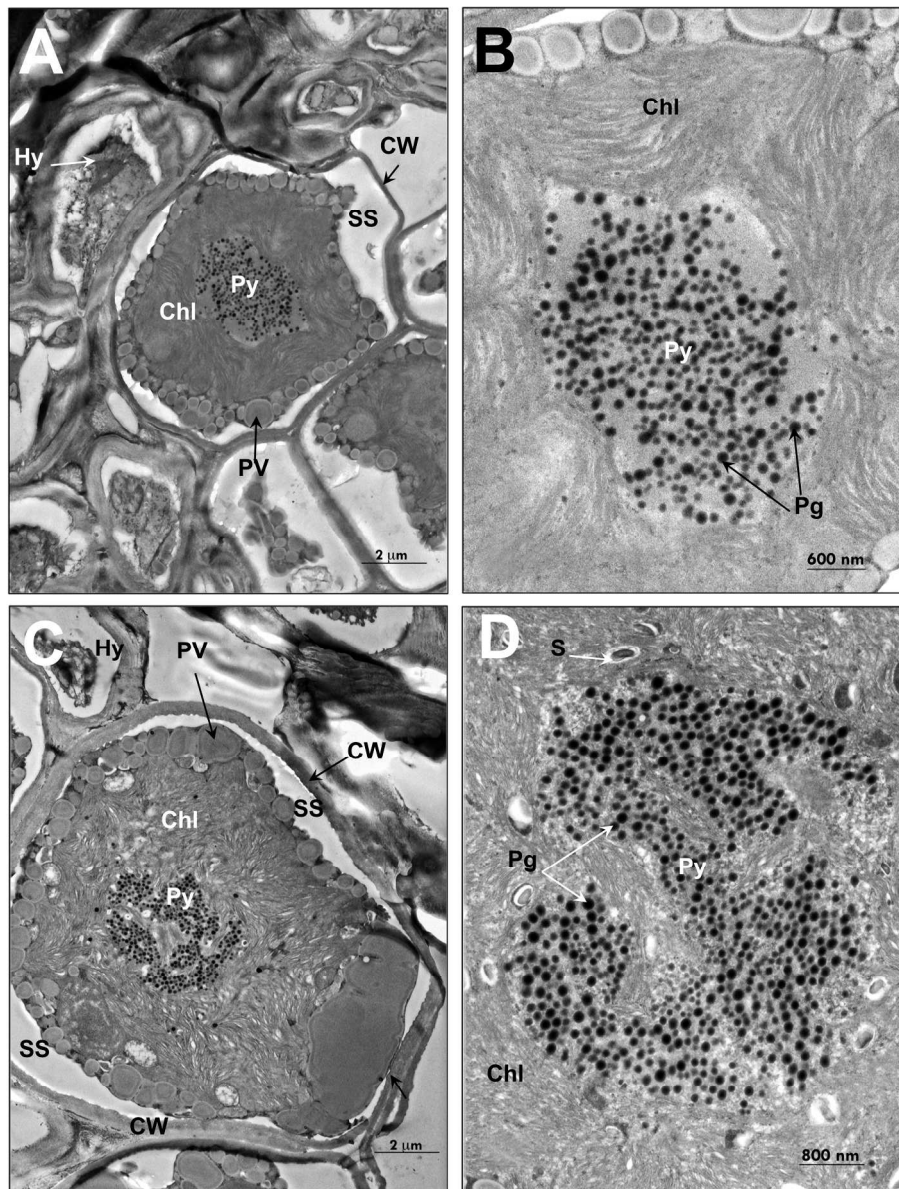
260x866mm (300 x 300 DPI)



251x328mm (300 x 300 DPI)



251x328mm (300 x 300 DPI)



251x327mm (300 x 300 DPI)

Table 1. GenBank accession number for specimens in this study and collector number. * Selected specimens for HTS analysis.

Sanger	Lichen species	Location	Code	nrITS DNA	nrITS DNA	LSU rDNA	Collector number
				mycobiont	phycobiont		
	<i>C. gyrosa</i>	Maranchón	1	MG979702	MH035928	MH035903	EB_07092014_A_0032
	<i>C. gyrosa</i>	Maranchón	2	MG979703	MH035929	MH035904	EB_07092014_A_0033
	<i>C. gyrosa</i>	Maranchón	3	MG979704	MH035930	MH035905	EB_07092014_A_0034
	<i>C. gyrosa</i>	Maranchón	4	MG979705	MH035931	MH035906	EB_07092014_A_0035
	<i>C. gyrosa</i>	Maranchón	5	MG979706	–	–	EB_07092014_A_0036
	<i>C. gyrosa</i>	Maranchón	6	MG979707	–	–	EB_07092014_A_0037
	<i>C. gyrosa</i>	Maranchón	7	MG979708	–	–	EB_07092014_A_0038
	<i>C. gyrosa</i>	Maranchón	8	MG979709	–	–	EB_07092014_A_0039
	<i>C. gyrosa</i>	Maranchón	9	MG979710	–	–	EB_07092014_A_0040
	<i>C. gyrosa</i>	Maranchón	10	MG979711	MH035932	MH035907	EB_07092014_A_0041
	<i>C. gyrosa</i> *	Maranchón	11	MG979712	MH035933	MH035908	EB_07092014_A_0042
	<i>C. sp. 'paramerae'</i>	Javalambre	1	MG979663	–	–	EB_11242009_0007
	<i>C. sp. 'paramerae'</i>	Javalambre	2	MG979664	MH035909	MH035884	EB_11242009_0008
	<i>C. sp. 'paramerae'</i>	Javalambre	3	MG979665	MH035910	MH035885	EB_11242009_0009
	<i>C. sp. 'paramerae'</i>	Javalambre	4	MG979666	MH035911	MH035886	EB_11242009_00010
	<i>C. sp. 'paramerae'</i>	Javalambre	5	MG979667	–	–	EB_11242009_00011
	<i>C. sp. 'paramerae'</i>	Javalambre	6	MG979668	–	–	EB_11242009_00012
	<i>C. sp. 'paramerae'</i>	Javalambre	7	MG979669	–	–	EB_11242009_00013
	<i>C. sp. 'paramerae'</i>	Javalambre	8	MG979670	–	–	EB_11242009_00014
	<i>C. sp. 'paramerae'</i> *	Javalambre	9	MG979671	MH035912	MH035887	EB_11242009_00015

Formatted Table

Formatted: Centered

Formatted Table

<i>C. sp. 'oromediterranea'</i>	Javalambre	1	MG979672	–	–	EB_11262009_0025
<i>C. sp. 'oromediterranea'</i>	Javalambre	2	MG979673	–	–	EB_11262009_0026
<i>C. sp. 'oromediterranea'</i>	Javalambre	3	MG979674	–	–	EB_11262009_0027
<i>C. sp. 'oromediterranea'</i>	Javalambre	4	MG979675	–	–	EB_11262009_0028
<i>C. sp. 'oromediterranea'</i>	Javalambre	5	MG979676	–	–	EB_11262009_0029
<i>C. sp. 'oromediterranea'</i>	Javalambre	6	MG979677	–	–	EB_11262009_0030
<i>C. sp. 'oromediterranea'</i>	Javalambre	7	MG979678	–	–	EB_11262009_0031
<i>C. sp. 'oromediterranea'</i>	Javalambre	8	MG979679	–	–	EB_11262009_0032
<i>C. sp. 'oromediterranea'</i>	Javalambre	9	MG979680	–	–	EB_11262009_0033
<i>C. sp. 'oromediterranea' *</i>	Javalambre	10	MG979681	–	–	EB_11262009_0034
<i>C. hispida</i>	Maranchón	1	MG979682	MH035913	MH035888	EB_07092014_A_0043
<i>C. hispida</i>	Maranchón	2	MG979683	MH035914	MH035889	EB_07092014_A_0044
<i>C. hispida</i>	Maranchón	3	MG979684	MH035915	MH035890	EB_07092014_A_0045
<i>C. hispida</i>	Maranchón	4	MG979685	MH035916	MH035891	EB_07092014_A_0046
<i>C. hispida</i>	Maranchón	5	MG979686	MH035917	MH035892	EB_07092014_A_0047
<i>C. hispida</i>	Maranchón	6	MG979687	MH035918	MH035893	EB_07092014_A_0048
<i>C. hispida</i>	Maranchón	7	MG979688	–	–	EB_07092014_A_0049
<i>C. hispida</i>	Maranchón	8	MG979689	MH035919	MH035894	EB_07092014_A_0050
<i>C. hispida</i>	Maranchón	9	MG979690	MH035920	MH035895	EB_07092014_A_0051
<i>C. hispida *</i>	Maranchón	10	MG979691	MH035921	MH035896	EB_07092014_A_0052
<i>C. hispida</i>	Zaorejas	1	MG979692	MH035922	MH035897	EB_07092014_B_0001
<i>C. hispida</i>	Zaorejas	2	MG979693	–	–	EB_07092014_B_0002
<i>C. hispida</i>	Zaorejas	3	MG979694	MH035923	MH035898	EB_07092014_B_0003
<i>C. hispida</i>	Zaorejas	4	MG979695	MH035924	MH035899	EB_07092014_B_0004
<i>C. hispida</i>	Zaorejas	5	MG979696	MH035925	MH035900	EB_07092014_B_0005
<i>C. hispida</i>	Zaorejas	6	MG979697	–	–	EB_07092014_B_0006
<i>C. hispida</i>	Zaorejas	7	MG979698	MH035926	MH035901	EB_07092014_B_0007

	<i>C. hispida</i>	Zaorejas	8	MG979699	–	–	EB_07092014_B_0008
	<i>C. hispida</i>	Zaorejas	9	MG979700	–	–	EB_07092014_B_0009
	<i>C. hispida</i>	Zaorejas	10	MG979701	MH035927	MH035902	EB_07092014_B_0010

HTS	Lichen species	OTU	n° sequences	nrITS DNA phycobiont
	<i>C. gyrosa</i> Maranchon 11	1	4726	MH035961
	<i>C. gyrosa</i> Maranchon 11	2	13	MH035962
	<i>C. gyrosa</i> Maranchon 11	3	10	MH035963
	<i>C. gyrosa</i> Maranchon 11	4	8	MH035964
	<i>C. gyrosa</i> Maranchon 11	5	5	MH035965
	<i>C. gyrosa</i> Maranchon 11	6	5	MH035966
	<i>C. gyrosa</i> Maranchon 11	7	3	MH035967
	<i>C. gyrosa</i> Maranchon 11	8	3	MH035968
	<i>C. gyrosa</i> Maranchon 11	9	2	MH035969
	<i>C. gyrosa</i> Maranchon 11	10	2	MH035970
	<i>C. gyrosa</i> Maranchon 11	11	2	MH035971
	<i>C. sp. 'paramerae'</i> Javalambre 9	1	1956	MH035935
	<i>C. sp. 'paramerae'</i> Javalambre 9	2	9	MH035936
	<i>C. sp. 'paramerae'</i> Javalambre 9	3	6	MH035937
	<i>C. sp. 'paramerae'</i> Javalambre 9	4	4	MH035938
	<i>C. sp. 'paramerae'</i> Javalambre 9	5	10	MH035939
	<i>C. sp. 'paramerae'</i> Javalambre 9	6	4	MH035940
	<i>C. sp. 'paramerae'</i> Javalambre 9	7	6	MH035941

	<i>C. sp. 'paramerae'</i> Javalambre 9	8	2	MH035942
	<i>C. sp. 'oromediterranea'</i> Javalambre 10	1	4102	MH035943
	<i>C. sp. 'oromediterranea'</i> Javalambre 10	2	657	MH035944
	<i>C. sp. 'oromediterranea'</i> Javalambre 10	3	507	MH035945
	<i>C. sp. 'oromediterranea'</i> Javalambre 10	4	65	MH035946
	<i>C. sp. 'oromediterranea'</i> Javalambre 10	5	59	MH035947
	<i>C. sp. 'oromediterranea'</i> Javalambre 10	6	35	MH035948
	<i>C. sp. 'oromediterranea'</i> Javalambre 10	7	30	MH035949
	<i>C. sp. 'oromediterranea'</i> Javalambre 10	8	18	MH035950
	<i>C. sp. 'oromediterranea'</i> Javalambre 10	9	16	MH035951
	<i>C. sp. 'oromediterranea'</i> Javalambre 10	10	7	MH035952
	<i>C. sp. 'oromediterranea'</i> Javalambre 10	11	5	MH035953
	<i>C. sp. 'oromediterranea'</i> Javalambre 10	12	5	MH035954
	<i>C. sp. 'oromediterranea'</i> Javalambre 10	13	2	MH035955
	<i>C. hispida</i> Maranchon 10	1	1416	MH035956
	<i>C. hispida</i> Maranchon 10	2	6	MH035957
	<i>C. hispida</i> Maranchon 10	3	5	MH035958
	<i>C. hispida</i> Maranchon Zaorejas 10	1	966	MH035959
	<i>C. hispida</i> Maranchon Zaorejas 10	2	636	MH035960

Table 2. Summary of number of sequences of *Trebouxia* spp. obtained by pyrosequencing for each particular OTU in the five analyzed thalli. (S) indicates the primary phycobiont detected by Sanger sequencing, and (P) the most abundant by 454-pyrosequencing. The new OTUs are highlighted in grey.

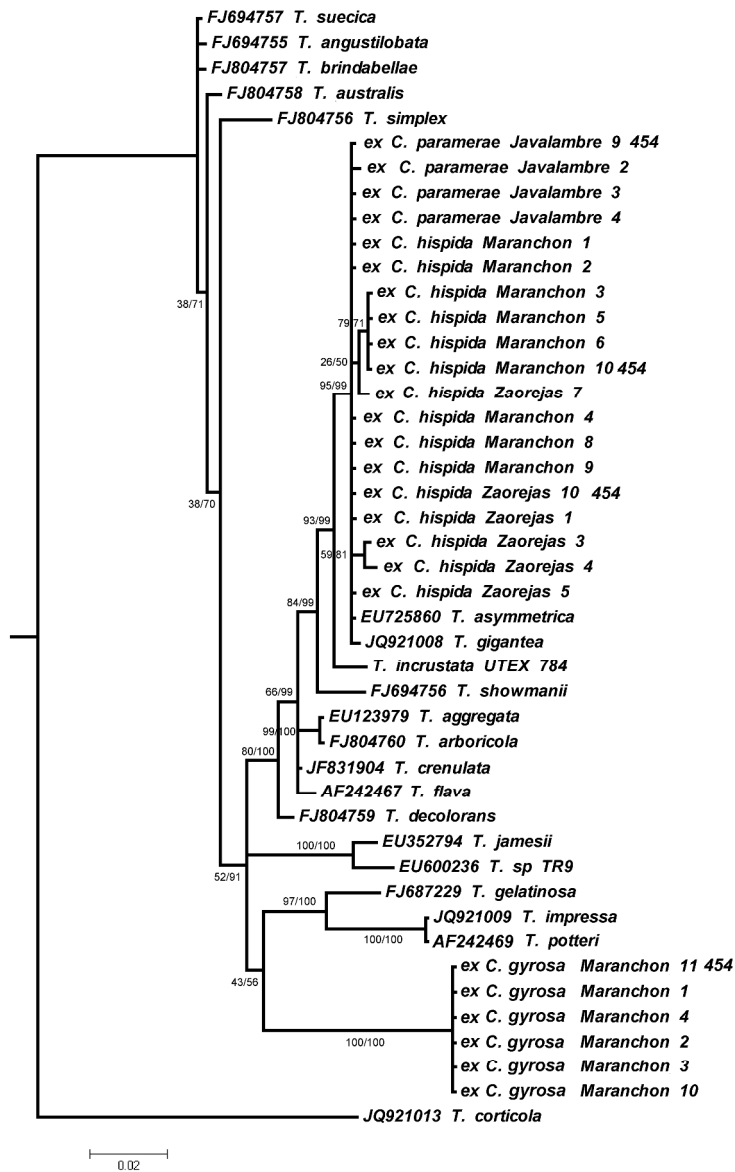
		<i>C. gyrosa</i>	<i>C. hispida</i> Zaorejas	<i>C. hispida</i> Maranchón	<i>C. 'oromediterranea'</i>	<i>C. 'paramerae'</i>
Clade I	I51	8(S/P)			35	
	I52					4
Clade S	S02	3			5	
	S08					2
	S51	4726 (S/P)				
	S52	2				
Clade A	<i>T. sp. Tr9</i>	13			16	
	<i>T. decolorans</i>	3				6
	<i>T. solaris</i>	2				
	<i>T. vaga</i> AV091			6		10
	<i>T. vaga</i> AV092	5				
	<i>T. asymmetrica</i>	5			507	
	<i>T. cretacea</i>	2	966 (P)	1416 (S/P)	59	
	A12		636 (S)		4102 (P)	1966 (S/P)
	A18				18	
	A21				5	
	A57			5		9
	A58				2	
	A59				65	
	A60	<u>*10</u>			30	
	A61				7	
	A62				657	
TOTAL OTUs		11	2	3	13	6

Table 3. Taxonomic identification of the *Asterochloris* sp. and additional green microalgae according to BLAST matches in the GenBank and numbers of the corresponding sequences present in each treatment.

	<i>Circinaria</i> spp.	OTUs	Blast Match	Query Coverage	Identity
<i>Asterochloris</i> sp.	<i>C. sp. 'paramerae'</i>	OTU9_4	<i>A. mediterranea</i> (KP257366)	100%	98%
	<i>C. sp. 'oromediterranea'</i>	OTU14_4	<i>A. mediterranea</i> (KP257366)	100%	99%
	<i>C. gyrosa</i>	OTU12_2	No significant similarity found		
Additional green microalgae	<i>C. sp. 'oromediterranea'</i>	OTU15_14	No significant similarity found		
	<i>C. sp 'oromediterranea'</i>	OTU16_40	Chlorophyta sp. URa19 (KF907687)	89%	100%
	<i>C. sp 'oromediterranea'</i>	OTU17_7	No significant similarity found		
	<i>C. gyrosa</i>	OTU13_45	No significant similarity found		
	<i>C. gyrosa</i>	OTU14_4	<i>Elliptochloris subsphaerica</i> (LT560353)	100%	96%
	<i>C. gyrosa</i>	OTU15_2	No significant similarity found		
	<i>C. gyrosa</i>	OTU16_18	Chlorophyta sp. URa19 (KF907687)	100%	97%

Table 4. Morphological characteristics of three morphotypes

		Pyrenoid measurements (Py)	Pyrenoid type	Cell diameter	Cell wall measurements (CW)	Cell wall layers	Peripheral vesicles (PV)	Citoplasmic inclusions (CI)	Starch (S)
Morphotype 1	<i>C. gyrosa</i>	3.5 ± 0.2 x 4.9 ± 0.4 μm	horseshoe shape	10.9 ± 1.1 μm	310.05 ± 20.31 nm	2	+	-	-
Morphotype 2	<i>C. sp. oromediterranea</i>	3.1 ± 0.8 x 2.0 ± 0.3 μm	<i>gigantea/ impressa</i>	8.7 ± 1.3 μm	330 ± 34.6 nm	3	+	+	-
	<i>C. sp. 'paramerae'</i>	2.3 ± 0.2 x 2.01 ± 0.05 μm	<i>gigantea/ impressa</i>	8.25 ± 1.35 μm	297 ± 47.1 nm	3	+	-	-
	<i>C. hispida</i> Zaorejas morphotype A	3.06 ± 0.95 x 2.9 ± 0.70 μm	<i>gigantea/ impressa</i>	8 ± 1.4 μm	228.74 ± 29.48 nm	3	+	-	-
Morphotype 3	<i>C. hispida</i> Zaorejas morphotype B	14.05 ± 1.4 mm	Irregular and lobulated	7 ± 0,54 μm	546.4 ± 97.3 nm	3	+	-	+
	<i>C. hispida</i> Maranchón	4.1 ± 0.8 x 3.1 ± 1.0 μm	Irregular and lobulated	11.4 ± 1.0 μm	434 ± 35,2 nm	3	+	+	+



260x390mm (300 x 300 DPI)